

## STEREOCHEMICAL AND ELECTRONIC CONTRIBUTIONS TO $^2E$ CHROMIUM(III) EXCITED STATE RELAXATION BEHAVIOR AT 77K

John F. Endicott, Ronald B. Lessard, Daniel Lynch, Marc W. Perkovic and Chong K. Ryu  
Department of Chemistry, Wayne State University, Detroit, MI 48202

### ABSTRACT

Variations in the radiative rate constants,  $k_r$ , for the  $^2E$  emission of chromium(III) am(m)ine complexes span at least a 78-fold range and are determined by spin-orbit coupling to the nearest quartet excited states. The 77K lifetimes of most of the (N-H) perdeuterated complexes are found to be correlated with the same spin-orbit coupling parameters. The notable exception found to this correlation is the N-H deuterated 1,2-bis (1,4,7-triaza-1-cyclononyl)ethane-chromium(III),  $\text{Cr}([9\text{JaneN}_3)_2\text{Et}^{3+}$ , complex for which the observed lifetime at 77K is 15% of that predicted by correlation with other am(m)ine complexes. This exception demonstrates that some low frequency mode mediated, non-radiative relaxation pathway can contribute to relaxation of the  $^2E$  excited state of Cr(III) complexes. The exceptional photophysical behavior of this complex extends to its emission spectra which are broad and matrix sensitive. It is postulated that the  $^2E$  excited state of  $\text{Cr}([9\text{JaneN}_3)_2\text{Et}^{3+}$  is distorted owing to the tendency of the bis-macrocyclic ligand to twist towards a prismatic geometry. It is inferred that variations in the electronic coupling matrix elements account for much of the variation in 77K ( $^2E$ )Cr(III) lifetimes.

### INTRODUCTION

The use of transition metal excited states as chemical reagents or as energy transducers necessitates a good understanding of the processes which unproductively deactivate these species, degrading the electronic excitation energy into heat. The excited state behavior of transition metal complexes has been especially challenging since there are generally many pathways for excited state relaxation. Some relationships between complex structure and excited state lifetimes are evolving for the  $^2E$  excited states of chromium(III) (refs. 1-4). However, even for ( $^2E$ )Cr(III) species the picture is complicated under ambient conditions with the matrix (i.e., solvent, crystal lattice, etc.) mediating much of the excited state relaxation behavior at room temperature (refs. 1-4). In principle, if such molecular properties as stereochemistry and electronic structure do directly influence excited state relaxation the way in which these influences alter the low temperature excited state relaxation rates should be relatively clear. It has been especially difficult to evaluate the excited state-ground state ( $^2E\text{-}^4A_2$ ) electronic coupling, and the influence of this coupling on excited state lifetimes.

The  $^2E$  excited state lifetimes of Cr(III) complexes tend to approach values,  $\tau_{\text{lim}}$ , at low temperatures (refs. 1-4). These limiting lifetimes thus seem to be true molecular properties, yet their variations, spanning a range of more than  $10^3$  (refs. 1-4), have been difficult to correlate with variations in simple structural parameters. For example, high frequency vibrational modes (e.g., O-H or N-H stretching frequencies) associated with coordinated atoms are effective in quenching the  $^2E$  excited states (refs. 1-11), but the expected (refs.12-15) dependence of  $\tau_{\text{lim}}$  on

the number of coupled high frequency acceptor modes,  $d_m$ , has been difficult to demonstrate over a variety of complexes (refs. 4, 5, 8). Thus simple correlations of  $\tau_{lim}$  with the number of high frequency oscillators,  $N_H$ , generally fail for large classes of complexes. On the other hand correlations of the form of equation (1) seem to work relatively well (Fig. 1)

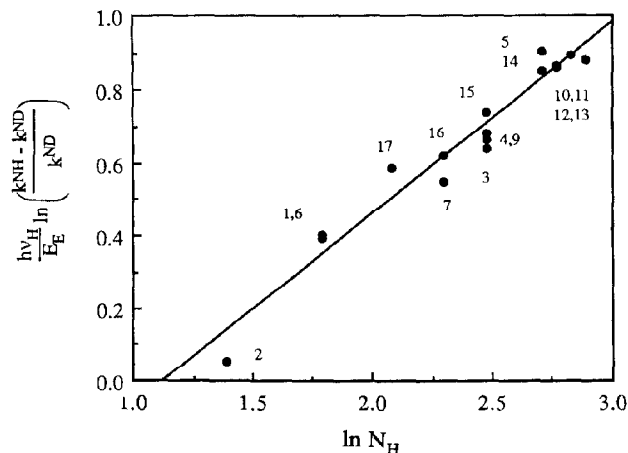


**Figure 1.** Illustration of the dependence of non-radiative relaxation rates of  $(^2E)Cr(III)$ -am(m)ine complexes on the number of coordinated high frequency oscillators ( $N_H$ ). The 77K data were taken from Table I of Ref. 16, and are numbered as in that table. The mean lifetime of (NH) protiated complexes is designated  $k_{NH}$ ; of (ND) deuterated complexes,  $k_{ND}$ ;  $h\nu_H$  taken to be the measured IR (NH) stretching frequency;  $E_E$  = electronic origin of  $^2E$  emission.

$$\ln[(k^{NH} - k^{ND})/k^{ND}] = a \ln N_H + b \quad (1)$$

(for  $k^{NH}$  and  $k^{ND}$  the inverse values of  $\tau_{lim}$  for protiated (NH) and perdeuterated (ND), respectively, am(m)ine complexes) (ref. 16). While equation (1) seems to be useful for most simple am(m)ine complexes, it does not correlate data reported for fluoro-am(m)ine complexes and there are appreciable deviations for cyano-am(m)ines. Furthermore, there are large variations in  $\tau_{lim}$ , even when high frequency accepting modes are absent (refs. 1-4, 16), and there seem to be no good criteria for relating these variations to structural parameters.

In general, one would expect the rate of excited state relaxation to be the sum of the contributions from competing pathways. In the simplest form, the mean relaxation rate constant can be represented as the sum of the rate constants for radiative relaxation,  $k_r$ , non radiative relaxation mediated by high frequency vibrational modes,  $k_{nr}^{hf}$ , and possible contributions from non-radiative relaxation pathways not involving high frequency modes,  $k_{nr}^{lf}$ , as in equation (2).

$$(\tau_{lim})^{-1} = k_r + k_{nr}^{hf} + k_{nr}^{lf} \quad (2)$$

The low frequency pathways are a special concern for d-d excited states since metal-ligand angular motions couple strongly with the metal centered d-orbitals, and such motions could facilitate the relaxation of the Laporte selection rules. However, there has been no clear demonstration, prior to this work, that  $k_{nr}^{hf}$  is ever much greater than  $k_r$ . It is convenient to factor the non-radiative relaxation rate constants into separate contributions from the electronic and nuclear constraints on the transition involved (Born-Oppenheimer approximation); the semi-classical form, equation (3), is

$$k_{nr}^i = \kappa_{el}^i \kappa_{nu}^i \nu_{eff}^i \quad (3)$$

useful for our further discussion ( $i = hf$  or  $lf$ ), where  $\kappa_{el}$  is an electronic retardation factor (or transmission coefficient),  $\kappa_{nu}$  is a nuclear retardation factor and  $\nu_{eff}$  is the frequency of the unrestricted transition. The observation that a simple rate ratio, such as equation (1), seems to improve the quality of the correlation between  $(\tau_{lim})^{-1}$  and  $N_H$  suggests that  $\kappa_{el} < 1$  for the non-radiative processes, and that it contributes a great deal to the variations in  $\tau_{lim}$ .

One expects the electronic coupling between the ground and excited state to be most unequivocally manifested in  $k_r$ . In this report we consider the information regarding the influence of electronic coupling on  $\tau_{lim}$ , and this has necessitated the determination of some values of  $k_r$ , the evaluation of their variations and the implications for electronic contributions to  $k_{nr}^i$ .

#### OBSERVED VARIATION IN THE (2E)CHROMIUM(III) RADIATIVE RELAXATION RATES AT 77K

There have been surprisingly few systematic studies and there are many difficulties. Most of the published work and most of the problems are discussed in Forster's recent review (ref.4). We have tried to make our determinations in a consistent medium (DMSO/H<sub>2</sub>O glass). While the determinations of  $\tau_{lim}$  are reasonably straightforward, determinations of  $k_r$  are subject to many errors (e.g., see refs. 4 and 17). We have devised a method, outlined below, for the determination of relative values of the radiative yields (more correctly the relative values of  $\eta_D k_r$  where  $\eta_D$  is the intersystem crossing efficiency of the Cr(III) complex). Relative yields are sufficient for many of our purposes.

##### The relative emission rate measurements.

Samples dissolved in 100 ml high purity DMSO/H<sub>2</sub>O (57:43, V:V) containing 0.1 g NaClO<sub>4</sub> were placed in a 1.2 cm i.d., 28 cm long pyrex tube, degassed and immersed in liquid nitrogen. Measurements were only made on clear glasses. The sample cell was lowered into a cylindrical quartz dewar so that the excitation beam traversed it 1.5 cm from its base. This apparatus was adjusted so that the laser beams reflected from the front and rear surfaces were colinear with the incident beam. Once the sample tube was aligned, the solution absorbance at the excitation wavelength and the emission intensity were determined.

A Molelectron UV-1010 nitrogen pumped Molelectron DL-14 dye laser (pulse width at half maximum = 10 ns) was employed as the light source with the laser dyes coumarin 440, BIS-MSB and DPS employed for excitations at 449, 420 and 407 nm respectively.

For the determination of sample absorbance, the laser beam was passed through a glass filter (Hoya B390) to remove background fluorescence of the dye laser. A 2 mm aperture 3 m from the dye laser resulted in a well collimated, homogeneous output beam. A plano-convex lens ( $f = 40$  cm) focussed this beam through the sample to a spot just behind the dewar, and a second plano-convex lens ( $f = 5$  cm) tightly focussed the transmitted light (of intensity  $I_{tr}$ ) onto a Molelectron J-3 pyroelectric joulemeter. The joulemeter output was passed through an Ortec Model 535 amplifier (10x gain) to a Gould-Biomation model 4500 transient recorder. The peak voltage of the joulemeter (50  $\mu$ s mean signal lifetime) is proportional to the total energy of the incident photons ( $Nh\nu$ ) and was recorded 3  $\mu$ s after firing the laser. Each determination was the average of 64 laser shots. The incident light intensity,  $I_0$ , was determined using the same apparatus and procedures, but with the sample cell containing only the glassy solvent. The intensity of light absorbed by the solution,  $I_a$ , could be obtained from,

$$I_a = I_0 - I_{tr} = I_0 (1 - 10^{-A})$$

where the instantaneous intensities are proportional to the voltage readings for a given excitation wavelength, and the number of photons absorbed can be obtained from the voltage readings:  $\Delta V/h\nu_{ex} = \gamma (n_a)$ ; where  $\Delta V = V_o - V_{tr}$ . Ambient absorbance readings using this procedure were within 0.002 absorbance units of those determined using a Perkin-Elmer Lambda 3B UV/VIS spectrophotometer.

Emitted light was collected and collimated at  $90^\circ$  to the excitation beam using a plano-convex lens ( $f = 7$  cm). The collimated beam was passed through a 70 cm long tube containing a  $K_2CrO_4/K_3[Fe(CN)_6]$  filter solution (greater than or equal to 92% transmittance for  $\lambda > 525$  nm) and focussed by means of planoconvex lens ( $f = 15$  cm) onto a red sensitive PMT (Hamamatsu model R928) biased at - 800 V. The PMT output was transmitted to the Gould-Biomation 4500 which had a digitization rate of 1 sample/10 ns. No correction was made for PMT wavelength response since most of the intensity of the  $(^2E)Cr(III)$  emissions occur over a narrow spectral range at 77K. The temporal and linear responses of the PMT were checked. The "instantaneous" intensity of emission,  $I_r$ , was recorded at 100 ns after the leading edge of the scattered laser light. The relative emission rate constants could then be obtained from,

$$\eta_D k_r' = m(I_r/I_a) = mI_r/(V_o - V_{tr})$$

where  $m$  and  $m'$  are system constants and  $I_r = \eta_D k_r \tau_{lim} I_a = \eta_D \phi_r I_a$ . The system constants were established for each excitation wavelength relative to  $Cr([9]aneN_3)_2^{3+}$ .

Results. Values of  $\eta_D k_r'$  for several complexes are listed in Table I.

**Table 1.** Photophysical parameters of some Cr(III) Complexes

Complex	$\eta_D k_f^a$	$\tau_{\text{lim}}^{\text{NH}}$ $\mu\text{s}$	$\tau_{\text{lim}}^{\text{ND}}$ $\mu\text{s}$	$E(^2E^0)$ $\text{cm}^{-1}/10^3$	$E(^4T_1)^{\text{max}}$ $\text{cm}^{-1}/10^3$	$\Delta\nu_{1/2}^b$ $\text{cm}^{-1}/10^3$	$\epsilon^b$ $\text{cm}^{-1}\text{M}^{-1}$
Cr(OAc) <sub>3</sub> [9]aneN <sub>3</sub>	4.7±0.9		395	13.99	19.53	3.51	340
Cr([9]aneN <sub>3</sub> ) <sub>2</sub> Et <sup>3+</sup>	2.9±0.2	50	114	13.67	20.79	3.82	280
cis-Cr(rac-(5,12)-Me <sub>6</sub> [14]aneN <sub>4</sub> )(CN) <sub>2</sub> <sup>+</sup>	1.7±0.3	207	1860	13.79	21.64	5.0	110
Cr([9]aneN <sub>3</sub> ) <sub>2</sub> <sup>3+</sup>	1	400	3030	14.72	22.80	3.22	89
trans-Cr([15]aneN <sub>4</sub> )(CN) <sub>2</sub> <sup>+</sup>	0.38±0.09	189		13.90	22.1	3.0	(60)
Cr(NH <sub>3</sub> ) <sub>5</sub> CN <sup>2+</sup>	0.36±0.07	100	7460	14.66	22.17	3.3	42.6
trans-Cr([14]aneN <sub>4</sub> )(CN) <sub>2</sub> <sup>+</sup>	0.06±0.04	394	3030	14.07	24.16	3.84	62.5
Cr(en) <sub>3</sub> <sup>3+</sup>	0.73 <sup>c</sup>	120 <sup>c</sup>	3030	14.92	21.84	3.2	85.9
Cr(NH <sub>3</sub> ) <sub>6</sub> <sup>3+</sup>	0.44 <sup>c</sup>	78 <sup>c</sup>	5320	15.23	21.64	3.34	43
Cr(tn) <sub>3</sub> <sup>3+</sup>	0.61 <sup>c</sup>	138 <sup>c</sup>	4760	15.02			
Cr(dim) <sub>2</sub> <sup>3+</sup>	1.05 <sup>c</sup>	208 <sup>c</sup>	4170	14.99	21.19	3.3	64
cis-Cr([14]aneN <sub>4</sub> )en <sup>3+</sup>	1.66 <sup>c</sup>	135 <sup>c</sup>	2220	14.78	21.48	3.4	136

Notes for Table 1

<sup>a</sup> Radiative rates relative to Cr([9]aneN<sub>3</sub>)<sub>2</sub><sup>3+</sup>. Error limits are 90% confidence limits based on replicate determinations. <sup>b</sup> Measurements made at 298 K. <sup>c</sup> Data from refs. 5 and 6. **Ligand abbreviations:** OAc<sub>3</sub>[9]aneN<sub>3</sub> = 1,4,7-tris(acetato)1,4,7-triazacyclononane; ([9]aneN<sub>3</sub>)<sub>2</sub>Et = 1,2-bis(1,4,7-triaza-1-cyclononyl)ethane; [9]aneN<sub>3</sub> = 1,4,7-triazacyclononane; rac-(5,12)-Me<sub>6</sub>[14]aneN<sub>4</sub> = 5,12-racemic-5,7,7,12,14,14-hexamethyl-1,4,8,11-tetraazacyclotetradecane; [15]aneN<sub>4</sub> = 1,4,8,12-tetraazacyclotetradecane; [14]aneN<sub>4</sub> = 1,4,8,11-tetraazacyclotetradecane.

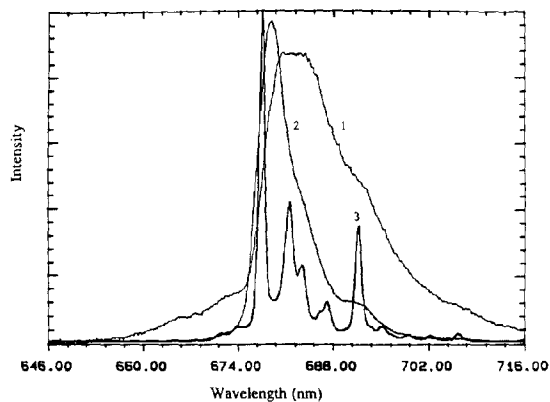


**Figure 2.** Emission spectra of  $[\text{Cr}([9]\text{aneN}_3)_2]\text{Cl}_3$  in different matrices: (1) DMSO/ $\text{H}_2\text{O}$  (1:1, V:V) fluid solution at 298K; (2) DMSO/ $\text{H}_2\text{O}$  (1:1, V:V) glass at 77K; (3) crystalline solid at 77K.

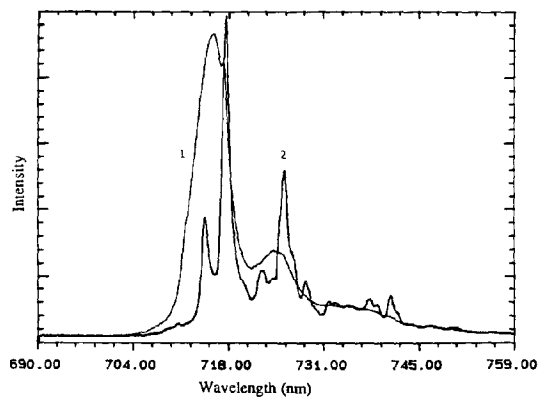


**Figure 3.** Comparison of 77K emission spectra of  $\text{Cr}(\text{OAc}_3[9]\text{aneN}_3)$  in: (1) DMSO/ $\text{H}_2\text{O}$  (1:1, V:V); and, (2) pure solid.

## EMISSION SPECTRA AND LIFETIMES.

Emission spectra were determined using either the Princeton Applied Research OMA-1 with SIT vidicon detector and On Line Instruments Systems, Inc. (OLIS) software as described elsewhere (refs 16, 18), or a Princeton Instruments IRY-512 diode array system. Emission lifetimes were determined using the Gould-Biomation 4500, OLIS software and a R955 PMT as described previously (refs. 16, 18). The Molelectron UV 1010 pumped DL-14 dye laser output was used for excitation in both kinds of measurement. Values of  $\tau_{\text{lim}}$  the  $^2E$  electronic origins ( $E^0$ ) are included in Table I.

While the ( $^2E$ )Cr(III) emission lifetimes tend to be nearly independent of the matrix at 77K if the Cr(III) complexes are reasonably dilute (glasses or doped crystalline solids), there are some striking variations in the emission spectra. Many, perhaps most Cr(III) complexes have very similar glassy solution and solid state (even the pure Cr(III) complex salts) spectra, but the band widths are greater for the spectra obtained from glassy solutions. The band shapes do differ in solutions and solid state for a few complexes, usually with enhanced intensity of the electronic origin accompanying the appreciable solution broadening of all components. This behavior was most noticeable for Cr([9]aneN<sub>3</sub>)<sub>2</sub><sup>3+</sup> (Fig. 2) and Cr(OAc<sub>3</sub>[9]aneN<sub>3</sub>) (Fig. 3). However, the emission found for Cr([9]aneN<sub>3</sub>)<sub>2</sub>Et<sup>3+</sup> was unique, among the complexes that we have examined, for its broad, relatively featureless emission, and the sensitivity of the band maximum to the solvent matrix (Fig. 4). Even more unusual, Cr([9]aneN<sub>3</sub>)<sub>2</sub>Et<sup>3+</sup> doped into [Rh([9]aneN<sub>3</sub>)<sub>2</sub>Et](PF<sub>6</sub>)<sub>3</sub> (1:30) exhibited two emission maxima (Fig. 5) at about 710 and 730 nm. The relative intensities of these maxima varied with the excitation wavelength through the low energy ( $\lambda_{\text{max}} = 480$  nm) ligand field absorption maximum as illustrated in Fig. 5.

## ELECTRONIC COUPLING AND ( $^2E$ )CR(III) RELAXATION RATES.

### The radiative rates.

The variations in the radiative rates of the spin and Laporte forbidden  $^2E \rightarrow ^4A_2$  transitions are in principle very straightforward (refs. 19, 20). The values of  $k_r$  should increase with: (1) decreases of the  $^2E - ^4T_2$  energy gap; and (2) decreases in complex symmetry.

The mean radiative rate constant for an allowed transition can be written (ref. 12),

$$k_r = B(\mu_{e \rightarrow g})^2 \sum_m (\nu_{0e \rightarrow gm})^3 \left| \int \Psi_{0e}^*(q) \Psi_{mg}(q) dq \right|^2 \quad (4)$$

where B is a collection of constants,  $\mu_{e \rightarrow g}$  (hereafter  $\mu_{eg}$ ) is the mean transition dipole moment,  $h\nu_{0e \rightarrow mg}$  is the energy of transition from the zeroth vibrational level of the excited state of the  $m^{\text{th}}$  vibrational level of the ground state, and the corresponding vibronic wavefunctions are integrated over the normal coordinates  $q$ . Strictly speaking, equation (4) is not correct for the  $^2E \rightarrow ^4A_2$  radiative rates, but it is a plausible basis for discussing the relative rates. The spin selection rule is relaxed through spin-orbit coupling of the  $^2E$  and  $^4T_2$  excited states (refs. 19, 20), the Laporte

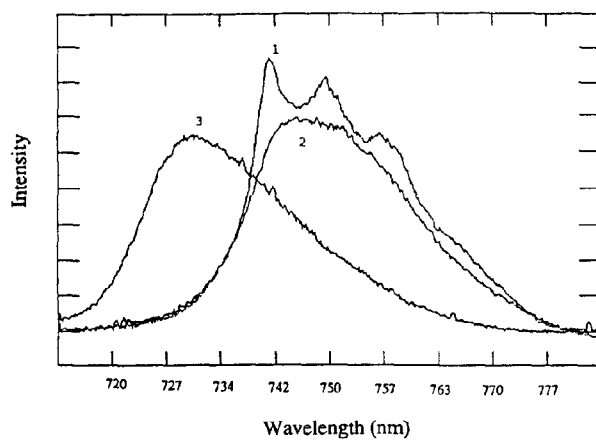


Figure 4. Emission spectra of  $[\text{Cr}([9]\text{aneN}_3)_2\text{Et}](\text{ClO}_4)_3$  in different matrices at 77K: (1) crystalline solid; (2) powder; (3) DMSO/ $\text{H}_2\text{O}$  (1:1, V:V).

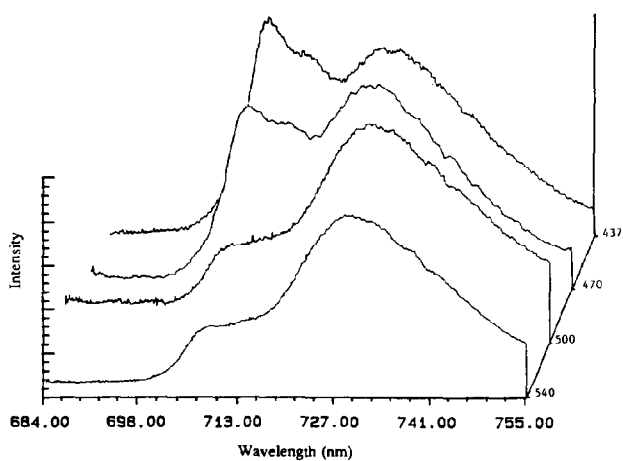


Figure 5. Excitation wavelength dependent luminescence of  $[\text{Cr}([9]\text{aneN}_3)_2\text{Et}]^{3+}$  doped (1:30) into solid  $[\text{Rh}([9]\text{aneN}_3)_2\text{Et}](\text{PF}_6)_3$  at 77K. Excitation wavelengths through the lowest energy absorption band are indicated along the right axis.



selection rule is relaxed in complexes without an inversion center or by means of coupling to symmetry reducing vibrations. One expects spin-orbit coupling to dominate the  ${}^2E \rightarrow {}^4A_2$  transition (refs. 19, 20), and this is most conveniently expressed in terms of the perturbational mixing of the zero-order doublet ( $\Psi_E^0$ ) and quartet ( $\Psi_T^0$ ) excited state wave functions,

$$\Psi_E = \Psi_E^0 + \frac{\langle \Psi_E^0 | \mathcal{H}_{so} | \Psi_T^0 \rangle}{(E_T - E_E)} \Psi_T^0$$

where  $\mathcal{H}_{so}$  is the spin-orbit Hamiltonian. Since  $\langle \Psi_A^0 | \mathcal{H} | \Psi_E^0 \rangle = 0$ , for  $\Psi_A^0$  the zero-order ground state wavefunction, only the spin-orbit terms contribute to equation (4) and the radiative relaxation rate constant has the form  $k_r({}^2E) = C_{so}k_r({}^4T_2)$ . The spin-orbit coefficient,  $C_{so}$ , may be expressed in terms of a spin-orbit coupling constant,  $\lambda$ , the energies of the quartet absorption ( $h\nu_T$ ) and doublet emission ( $h\nu_E$ ) maxima,  $\Delta E = (E_T - E_E)$  and the multiplicity ratio (refs. 19, 20),

$$k_r({}^2E) = \frac{4}{9} (\lambda/\Delta E)^2 (\nu_E/\nu_T) k_r({}^4T) \quad (5)$$

The radiative rate of the quartet may be written (ref. 12),

$$k_r({}^4T_2) = 3.06 \times 10^9 \nu_T^3 n^2 \epsilon_{\max} \Delta\nu_{1/2}/\nu_{\max} \quad (6)$$

where  $n$  is the index of refraction,  $\epsilon_{\max}$  is the molar extinction coefficient at the absorption maximum and  $\Delta\nu_{1/2}$  is the full width at half maximum. Thus, from equations (5) and (6) we expect a correlation of the form,

$$k_r({}^2E) \cong 1.4 \times 10^{-9} n^2 (\lambda/\Delta E)^2 \nu_E \nu_T^2 \epsilon_{\max} \Delta\nu_{1/2}/\nu_{\max} \quad (7)$$

To allow for the possibility that other terms might contribute to the transition probability (e.g., spin orbit coupling to other states, non-dipolar contributions to  $\mathcal{H}$ , etc.) we have plotted  $[\eta_D k_r'({}^2E)]^{1/2}$  vs  $[(\lambda/\Delta E) (\nu_E \nu_T^2 \epsilon_{\max} \Delta\nu_{1/2}/\nu_{\max})^{1/2}]$  in Fig. 6. However, there is no evidence for other contributions to  $k_r({}^2E)$ , and Fig. 6 demonstrates that the  $({}^2E)Cr(III)$  radiative relaxation dynamics are dictated by spin-orbit coupling between the  ${}^2E$  and  ${}^4T_2$  excited states. This correlation also indicates that  $\eta_D$  has very similar values in most of the  $Cr(III)$  complexes. The appreciably smaller value of  $\eta_D k_r'$  for  $({}^2E)Cr([14]aneN_4)(CN)_2^+$  than expected for the correlation in Fig. 6 could indicate that  $\eta_D$  is unusually small for this complex; however the signal was so weak in this particular determination that a strong inference is not justified.

## RELAXATION RATES OF THE PERDEUTERO COMPLEXES

In principle,  $(\tau_{lim}^{ND})^{-1} = k_r + k_{nr}^{lf}$ , where  $k_{nr}^{lf}$  represents non-radiative relaxation pathways mediated by low frequency vibrational modes. The limiting, low temperature non-radiative relaxation rates can be viewed as vibronically mediated tunneling processes. (refs. 12, 13). Even so, one expects some similarities between  $k_r$  and the electronic components (as manifested in  $\kappa_{el}$ ) of

$k_{nr}^i$  ( $i = hf$  or  $lf$ ). For example, the contribution to  $k_r$  of "intensity stealing" from spin-allowed transitions depends on the magnitude of the spin-orbit coupling constant,  $\lambda$ , and the energy separation of the coupled states,  $\Delta E$ , and the similar quantities are expected to contribute to  $\kappa_{el}$ .

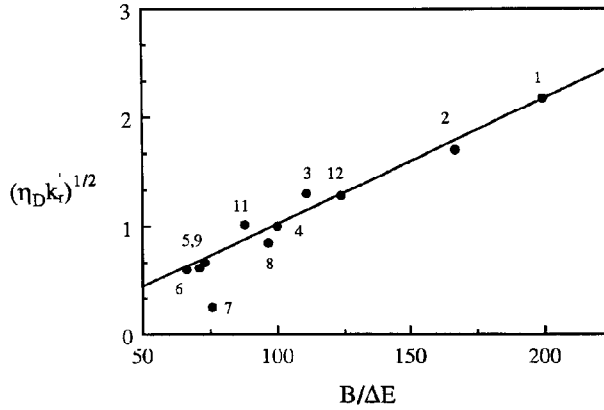


**Figure 6.** Dependence of the relative radiative emission rates  $(\eta_D k_r')^{1/2}$  on the energy difference ( $\Delta E$ ) between the  $^2E$  and lowest energy quartet (designated " $^4T_2$ ") excited states, modified by the relative oscillator strengths for the lowest energy quartet absorption ( $^4A_2 \rightarrow ^4T_2$ ) as predicted for spin orbit perturbational coupling of the  $^2E$  excited state with the  $^4A_2$  ground state;  $B = \lambda [v_E v_T \epsilon_{\max} \Delta v_{1/2} / v_{\max}]^{1/2}$ , where  $\lambda$  is the spin orbit coupling constant,  $v_E$  and  $v_T$  are the emission maxima doublet and (hypothetical) quartet emissions and  $\epsilon_{\max}$ ,  $v_{1/2}$  and  $v_{\max}$  are  $^4A_2 \rightarrow ^4T_2$  absorption parameters. Based on refs. 12, 20, 21. Points numbered according to the descending sequence in Table I.

## ELECTRONIC CONTRIBUTIONS TO THE NONRADIATIVE RATES

For an electronically forbidden non-radiative process  $\kappa_{el} \ll 1$  and can be expressed as (ref. 21).

$$\kappa_{el} \equiv [(2V_{if}^2/\hbar) (2\pi^3/E_{nu}\hbar v_{nu})^{1/2}] / v_{eff}$$

where the electronic matrix element  $V_{if} = \langle \Psi_f | \mathcal{H}' | \Psi_i \rangle$ ,  $\mathcal{H}'$  is the Hamiltonian term which induces the transitions,  $E_{nu}$  is the energy of the nuclear displacements which accompany the transition ( $E_{nu} \equiv$  one half the Stokes-shift) and  $v_{nu}$  is the associated nuclear frequency. For the  $^2E \rightarrow ^4A_2$  non-radiative transition, one might expect spin-orbit coupling to dominate so that  $\mathcal{H}' \equiv \mathcal{H}_{so}$  and  $V_{if}$  to be approximately of the form (ref. 15),

$$V_{if} \equiv \sum_j \langle \Psi_T | \mathcal{H}_{so} | \Psi_E \rangle / \Delta E \rangle J_{EA}$$

where  $J_{jEA}$  is the vibronic coupling constant which describes the electron-nuclear coupling for the promoting modes,  $j$ , which are effective in coupling the  ${}^2E$  excited state and the  ${}^4A_2$  ground state. For our purposes it is sufficient to treat  $\sum_j J_{jEA}$  as a constant,  $\beta'$ , for this series of complexes. Then,

$$k_{nr}^i \equiv (2/\hbar)\beta'(\lambda/\Delta E)^2(2\pi^3/E_{nu}h\nu_{nu})\kappa_{nu} \equiv \beta(\lambda/\Delta E)^2\kappa_{nu}$$

where all the constants or presumably slowly varying terms have been collected in  $\beta$ .

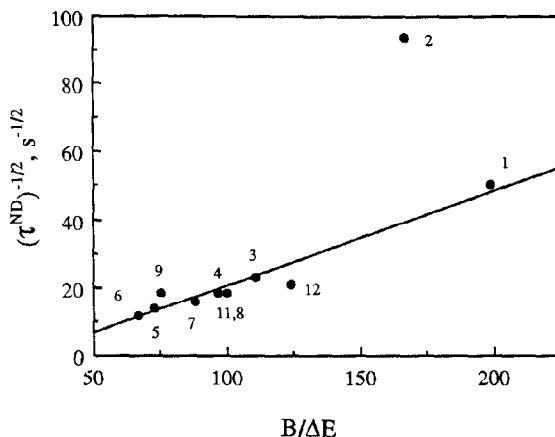


**Figure 7.** Comparison of inverse mean lifetimes of N-D perdeutero ( ${}^2E$ )Cr(III) excited states to radiative-spin-orbit coupling parameters;  $B$  and  $\Delta E$  as in Fig. 6.

Forster has recently (ref. 4) raised the possibility that  $(\tau_{lim}^{ND})^{-1}$  might be nearly equal to  $k_r$ . In accord with this view,  $(\tau_{lim}^{ND})^{-1}$  is not correlated simply with  $(\Delta E)^{-2}$ , as equation (7) suggests that it should be if  $k_{nr}^{lf}$  were much greater than  $k_r$ . Rather, Fig. 7 demonstrates a good correlation but not as good as the correlation of  $k_r$  in Fig. 6) of  $(\tau_{lim}^{ND})^{-1}$  with  $(\lambda/\Delta E)(vE\nu_T^2\varepsilon_{max}\Delta\nu_{1/2}/v_{max})^{1/2}$ , consistent with a very substantial contribution of  $k_r$  to  $(\tau_{lim}^{ND})^{-1}$  for most of the complexes. However, the form of the electronic matrix element contribution to  $k_{nr}^i$  is not known with sufficient certainty to base quantitative inferences about the relative magnitudes of  $k_{nr}^{lf}$  and  $k_r$  for most complexes on the correlation in Fig. 7. There is one outstanding exception:  $(\tau_{lim}^{ND})^{-1/2}$  for the  $Cr([9]aneN_3)_2Et^{3+}$  complex is nowhere close to the value based on the correlation line in Fig. 7. This strongly suggests that  $k_{nr}^{lf} \gg k_r$  for this complex. In view of this, it is very unlikely that  $k_r \gg k_{nr}^{lf}$  for all the other complexes, and much of the scatter of data around the correlation line in Fig. 7 could be the consequence of comparable contributions of  $k_r$  and  $k_{nr}^{lf}$  with their slightly different dependencies on system parameters. An exceptionally large value of  $k_{nr}^{lf}$  inferred for  $Cr([9]aneN_3)_2Et^{3+}$  would be consistent with an exceptionally, for ( ${}^2E$ )Cr(III), distorted excited

state resulting in a larger than usual probability for nuclear tunneling, i.e., the contribution of  $\kappa_{\text{nu}}$  is expected to increase with nuclear distortion. Thus, the  $^2\text{E}$  relaxation dynamics of  $\text{Cr}([\text{9}]\text{aneN}_3)_2\text{Et}^{3+}$  seem consistent with the unusual spectroscopic behavior of this complex discussed above.

#### EVALUATION OF THE POTENTIAL CONTRIBUTIONS OF STEREOCHEMICAL STRAIN TO EXCITED STATE DISTORTION IN $[\text{9}]\text{aneN}_3$ COMPLEXES.

We have used MM2 calculations to examine the possibility that the ligand might promote excited state distortion in  $\text{Cr}([\text{9}]\text{aneN}_3)_2\text{Et}^{3+}$ , but not in  $\text{Cr}([\text{9}]\text{aneN}_3)_2^{3+}$ . The Allinger-Yuh MM2 program (ref. 22), modified to include 6-8 coordinate metals has been used in these calculations. The calculational strategy was designed to assess the manner in which the amine ligands might affect the relaxation coordinate. To this end structures were minimized for different Cr-N "unstrained" bond lengths or N-Cr-N angles, but otherwise using standard interaction parameters (refs. 21, 22) (more detailed descriptions of our procedures see refs. 24, 25) and all interactions of the metal were removed from the total steric energy to obtain a residual (ligand) steric energy,  $\Delta E_s$ . For the unstrained Cr-N bond length of 2.03 Å, the ligands of both  $\text{Cr}([\text{9}]\text{aneN}_3)_2^{3+}$  and  $\text{Cr}([\text{9}]\text{aneN}_3)_2\text{Et}^{3+}$  would tend to twist slightly if there were no angular dependence of the Cr-N bond, but the tendency to twist is about 10 times larger in the  $\text{Cr}([\text{9}]\text{aneN}_3)_2\text{Et}^{3+}$  complex (Fig. 8): minima for a trigonal twist angle of 25° and  $\Delta(\Delta E_s) = -3 \text{ kcal mol}^{-1}$ , and 18° and  $-7 \text{ kcal mol}^{-1}$  respectively for the two complexes (30° for an octahedral geometry, 0° for trigonal prismatic). Furthermore, the preferred twist angle increases very dramatically when the Cr-N distance is increased from 2.0 to 2.2 Å in the  $\text{Cr}([\text{9}]\text{aneN}_3)_2\text{Et}^{3+}$  complex, but there is very little change in the preferred twist angle of  $\text{Cr}([\text{9}]\text{aneN}_3)_2^{3+}$  as the bond length is increased (Fig. 9). These calculations indicate that the coordinated  $[\text{9}]\text{aneN}_3)_2\text{Et}$  ligand is trigonally strained, and that it has a very distinct tendency to reduce this strain by promoting a trigonal distortion in its Cr(III) complex. In contrast, the parent bis- $[\text{9}]\text{aneN}_3$  complex is much less distorted and tends to impede large amplitude trigonal distortions.

The photophysical implications of these calculations are two-fold. First, since the population a quartet excited state by light absorption is expected to result in a large (about 0.1 Å) increase in the Cr-N bond length (ref. 26) and the vibrationally equilibrated ( $^4\text{T}_2$ ) $\text{Cr}([\text{9}]\text{aneN}_3)_2\text{Et}^{3+}$  excited state is predicted to undergo a large amplitude trigonal distortion while the ligands in the parent  $\text{Cr}([\text{9}]\text{aneN}_3)_2^{3+}$  complex would tend to hinder a simple twist for comparable bond length changes. Secondly, the presence of doubly occupied "t<sub>2g</sub>" orbital terms in the  $^2\text{E}$  wave function of a trigonally distorted complex (ref. 27) will tend to make the potential energy barrier to trigonal twisting smaller than would be the case for a more nearly octahedral complex.

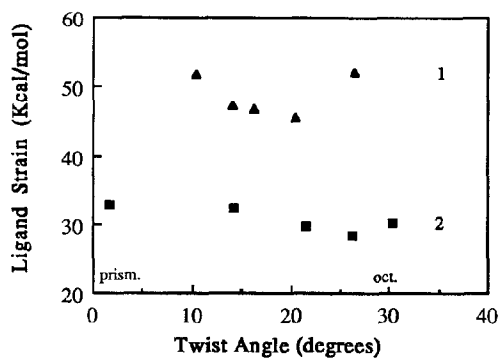


**Figure 8.** MM2 calculated variations of repulsive, ligand-ligand interactions with trigonal twist angle in 6-coordinate complexes: 1, for  $[9]\text{aneN}_3)_2\text{Et}$ ; 2, for  $[9]\text{aneN}_3)_2$ .

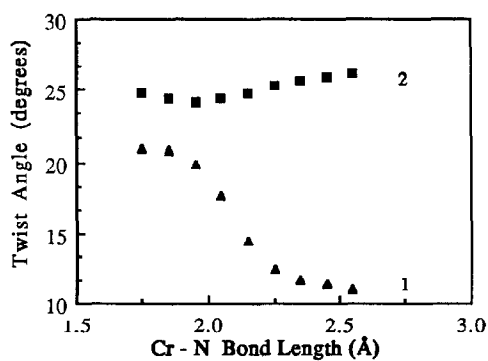


**Figure 9.** MM2 calculated variations in trigonal twist angle with the size of the coordination sphere in the 6-coordinate complexes with: (1) for  $[9]\text{aneN}_3)_2\text{Et}$ ; (2) for  $[9]\text{aneN}_3)_2$ .

## CONCLUSIONS

The photophysical and spectroscopic behavior of the  $\text{Cr}([\text{9}]\text{janeN}_3)_2\text{Et}^{3+}$  complex strongly suggest that its  $^2\text{E}$  excited state is unique among  $\text{Cr}(\text{III})$  systems in having a geometry different from that of the ground state. Molecular modeling suggests that the excited state distortion of this complex is a large amplitude twist towards a trigonal prismatic geometry.

The relative radiative rate constants for the  $^2\text{E}$  decrease as predicted with increase in the excited state  $^2\text{E} - ^4\text{T}_2$  energy gap (i.e.,  $k_r \propto (\Delta E)^{-2}$ ). The form of electronic matrix element contributions to the non-radiative rate constants is still unclear.

## ACKNOWLEDGEMENT

Partial support of this research by the Division of Chemical Sciences, Office of Basic Energy Sciences, Office of Energy Research, U. S. Department of Energy is gratefully acknowledged.

## REFERENCES

1. T.J. Kemp, *Progr. React. Kinet.*, 10 (1980) 301.
2. J.F. Endicott, T. Ramasami, R. Tamilarasan, R.B. Lessard, C.K. Ryu and G.R. Brubaker *Coord. Chem. Rev.*, 77 (1987) 1.
3. J.F. Endicott, R.B. Lessard, Y. Lei, C.K. Ryu and R. Tamilarasan in *Excited States and Reactive Intermediates*, A.B.P. Lever, Ed., ACS Symposium Series, No. 307, American Chemical Society, Washington, D.C., (1986) p. 85.
4. L.S. Forster, *Chem. Rev.*, submitted.
5. K. Kuhn, F. Wasgestian and H. Kupka, *J. Phys. Chem.*, 85, (1981) 665.
6. M. Muele and F. Wasgestian, *Inorg. Chim. Acta*, 119 (1986) 25.
7. A. Ditzel and F. Wasgestian, *Ber. Bunseng. Phys. Chem.*, 90 (1986) 111.
8. A.F. Fucaloro, L.S. Forster, J.V. Rund and S.H. Lin, *J. Phys. Chem.*, 87 (1983) 1796.
9. L.S. Forster and O. Monsted, *J. Phys. Chem.*, 90 (1986) 5131.
10. A.M. Gaith, L.S. Forster and J.V. Rund, *Inorg. Chem.*, 26 (1987) 2493.
11. D.J. Robbins and A.J. Thomson, *Mol. Phys.*, 25 (1973) 1103.
12. J.B. Birks, *Photophysics of Aromatic Molecules*, Wiley, New York, 1970.
13. J.T. Yardley, *Introduction to Molecular Energy Transfer*, Academic Press, New York, 1980.
14. R. Englman and J. Jortner, *Mol. Phys.*, 18 (1970) 145.
15. K.F. Freed and J. Jortner, *J. Chem. Phys.*, 52 (1970) 6372.
16. C.K. Ryu, R.B. Lessard, D. Lynch and J.F. Endicott, *J. Phys. Chem.*, 93 (1989) 1752.
17. J. Demas and G.A. Crosby, *J. Phys. Chem.*, 75 (1971) 991.
18. R.B. Lessard, J.F. Endicott, M.W. Perkovic and L.M. Ochromowycz, *Inorg. Chem.*, 28 (1989) 2574.

19. Y. Tanabe, Progr. Theoret. Phys. (Kyoto), Suppl., 14 (1960) 17.
20. S. Sugano, Y. Tanabe and H. Kaminura, Multiplets of Transition Metal Ions in Crystals, Academic Press, New York, 1970.
21. M.D. Newton and N. Sutin, Ann. Rev. Phys. Chem., 35 (1984) 437.
22. N.L. Allinger and Y.H. Yuh, QCPE 395 Molecular Mechanics; Operating Instructions for MM2 and MMP2 Programs 1977 Force Field, Quantum Chemistry Program Exchange, QCPE Program No. 395, Indiana University, Chemistry Dept., Bloomington, IN.
23. G.R. Brubaker and D.W. Johnson, Coord. Chem. Rev., 53 (1984) 1.
24. J.F. Endicott, K. Kumar, C.L. Schwarz, M.W. Perkovic and W. K. Lin, J. Am. Chem. Soc., 111 (1989) in press.
25. C.L. Schwarz and J.F. Endicott, Inorg. Chem., 28 (1989) in press.
26. R.B. Wilson and E.I. Solomon, Inorg. Chem., 17 (1978) 1729.
27. A. Ceulemans, N. Bongaerts and L.G. Vanquickenborne, Inorg. Chem., 26 (1987) 1566.